Modeling and analyzing autogenous shrinkage of hardening cement paste

Tianshi Lu[1*], Eddie Koenders[1,2]
(1) Delft University of Technology, Delft, The Netherlands
(2) Universidade Federal do Rio de Janeiro, Rio de Janeiro, Brazil

Abstract: In this paper, a conceptual model for analyzing the plastic part of autogenous deformation of cement paste based on the Arrhenius rate theory will be presented. The autogenous deformation will be calculated from the elastic deformations with inclusion of creep. Different kinds of cement paste with a water cement ratio 0.3 are tested and studied, and experimental result compare the model calculation. The results lead to the conclusion that early age creep plays a very important role in the autogenous deformation of hydrating cement paste and should not be neglected in simulation models.

Keywords: Autogenous shrinkage; Plastic deformation; Atthenius rate theory; Blended cement paste; Predictive models

1 Introduction

Autogenous deformation is the self-desiccating deformation of a cement paste, mortar or concrete that evolves during hardening. Changes in the surface tension of the solid gel particles, disjoining pressure, and tension in capillary water are the principal mechanisms that have been debated along with this issue[1]. Because cement paste is a visco-elastic-plastic material, the early age deformation caused by the internal driving force mentioned before, should be divided into three parts:

$$\varepsilon = \varepsilon^{p} + \varepsilon^{e} + \varepsilon^{c} \quad (1)$$

In which, ε is total autogenous deformation, ε^{p} is the early age plasticity before an initial network of (touching) cement particles has formed that can resist the early age deformation stress, ε^{e} is the elastic deformation, ε^{c} is the visco-elastic part, which is represented by creep.

During past few decades, elastic deformation induced by internal self-desiccating driving forces, e.g. capillary force, has been considered as the major source of early age autogenous deformation by several researchers[2-7]. However, simulations show that differences between the measured and calculated autogenous deformation are becoming more pronounced after the first 24 hours [2]. Even taking disjoining pressure and surface tension into consideration, the difference can only be partly explained. Therefore, creep must play an important role in early age autogenous deformation of hydrating cement paste, especially at the first seven days after final setting, when strength and elastic modulus of cement paste are still growing, cement paste behaves more like a visco-elastic material.

Since Arrhenius produced his equation in 1889[8] on the influence of temperature on the rate of inversion of sucrose, i.e. the concept that certain chemical reactions need to be supplied with an activation energy to proceed, this equation has also been applied to describe the behavior of numerous materials, including cement paste and concrete. Polivka and Best[9] pointed out that time-dependent deformation of concrete can occur only as a result of thermally activated molecular processes of deformation. Six years later Wittmann[10], using statistical thermodynamics, derived a relation between creep rate and applied static stress for concrete, which was similar to the one derived for metals.

This paper focuses on a model for autogenous deformation that includes a visco-elastic part which is based on the activation energy theory. For this, ordinary Portland cement paste (CEM I 42.5N) with and without 10% silica fume was studied. By combining the results with elastic and

* Corresponding author .Tel:+31152781662;E-mail address:T.Lu-1@tudelft.nl

visco-elastic deformations the effect of creep becomes clearly visible. The calculating results are compared with test results to verify the accuracy of the model.

2 Theoretical basis

2.1 Work-based modelling approach

For a one-way bearing situation, the work done during creep of cement paste under a constant permanent load is made up of an elastic component A_{el}, and a resistance component A_R

$$Fx = A_{el} + A_R \qquad (2)$$

In which, F is the load that causes the deformation and x is the deformation.

A_{el} is given by

$$A_{el} = V\int_0^{\varepsilon} \sigma d\varepsilon \qquad (3)$$

Assuming Hooke's Law, $\sigma = E\varepsilon$, then Eq. (3) becomes

$$A_{el} = V\int_0^{\varepsilon} E\varepsilon d\varepsilon = VE\frac{\varepsilon^2}{2} = Al\frac{E}{2}\frac{x^2}{l^2} = \frac{EA}{2l}x^2 \qquad (4)$$

Where A and l are the cross-section and length of the sample respectively.

Assuming the resistance component to be proportional to x and taking into consideration that it is also proportional to the number of points of contact in the cement gel and thus to the amount of hydrated cement $\alpha C'$, where C' equals the amount of initial cement per unit volume so that $C' = C/(W+C) = 1/(1+W/C)$, then

$$A_R = R'\alpha C' x\dot{x} \qquad (5)$$

Where R' is the constant of proportionality and α is the degree of hydration.

Therefore, Eq. (2) can be expressed as:

$$Fx = \frac{qE}{2l}x^2 + R'\alpha C' x\dot{x} \qquad (6)$$

Solving this equation leads to the creep function for cement paste, and can be expressed by:

$$\varepsilon(t) = \frac{2\sigma}{E}\left(1 - e^{-\frac{qE}{2lR'C'\alpha}t}\right) \qquad (7)$$

2.2 Activation energy

The quantity R', which is proportional to the internal friction, does not remain constant during the creep process, but increases with increasing deformation. In wittmann's paper[11] an attempt was made to determine how R' varies with activation energy. This method yields a useful result:

$$R' = \frac{C_1}{C''}e^{\frac{Q}{RT}} \qquad (8)$$

Where $C_1 = q\sigma/lC'\alpha$, C'' is the frequency factor, $C'' = a\sinh(b\sigma)$, Q is the experimental activation energy of the cement creep. Many papers have been published on the value of the experimental activation energy[8,10,11], the value vary with the material , water cement ratio, curing condition and many other factors. In this paper, the value around 39 KJ/mol has been taken.

Combining Eq.(7) and Eq.(8) we obtain

$$\varepsilon(t) = \frac{2\sigma}{E}\left(1 - e^{-\frac{EC''}{Q}t}\right) = \frac{2\sigma}{E}\left(1 - e^{-\frac{a\sinh(b\sigma)E}{Q}t}\right) \qquad (9)$$

For the three-way bearing situation, the Eq.(7) and Eq.(9) can be written as:

$$\varepsilon(t) = \frac{2\sigma}{E}(1-2\vartheta)\left(1 - 2\left(1 - e^{-\frac{qE}{2lR'C'\alpha}t}\right)\right) \qquad (10)$$

and

$$\varepsilon(t) = \frac{2\sigma(1-2\vartheta)}{E}\left(1 - e^{-\frac{EC''}{Q}t}\right) = \frac{2\sigma(1-2\vartheta)}{E}\left(1 - e^{-\frac{a\sinh(b\sigma)E}{Q}t}\right) \qquad (11)$$

2.3 Elastic deformation

For the one-way bearing situation, the elastic deformation ε^e in the Eq. (1) can be expressed as:

$$\varepsilon^e = \frac{\sigma}{E} \qquad (12)$$

σ is the stress, E is elastic modulus.

If the specimen is under three-dimensional stress, the elastic deformation ε^e in one certain direction can be expressed as :

$$\varepsilon^e = \frac{\sigma}{E}(1-2\vartheta) = \frac{\sigma}{3K_p} \qquad (13)$$

Where ϑ is the Poisson's ratio, K_p is bulk modulus.

2.4 Capillary tension

When the Kelvin radius is known, the tensile stress in the pore fluid can be calculated with the Laplace law, for circular cylindrical pores (assuming perfect wetting):

$$F_c = -\frac{2\gamma}{r} \qquad (14)$$

Where r is Kelvin radius and γ is the surface tension of the pore solutions filtered from the cement paste.

2.5 Effective stress

As mention before, the capillary tension in the pore fluid can be calculated as well. However, the applied stress $\sigma(t)$ and the physical property $E(t)$ mentioned in Eq.(11) are macroscale, while the internal driving force is microscale. If the autogenous deformation caused by the internal driving force, such as capillary stress, will be simulated by the macroscale Eq.(11), the concept of effective stress has to be introduced.

The effective stress σ_e [12], accounts for stress effects due to changes in porosity, spatial variation of porosity and deformations of the solid matrix, and may be written as a summation of the applied stress σ and the solid pressure p^s:

$$\sigma_e = \sigma + \kappa p^s I \qquad (15)$$

Where p^s is the solid phase pressure exerted by the pore fluids (liquid water and moist air), σ the applied stress tensor, I the unit tensor of second order, and

$$\kappa = 1 - K_p/K_S \qquad (16)$$

is the Biot coefficient accounting for different values of bulk moduli for solid phase (grain) and the skeleton, K_S and K_p. In Eq. (15). applied stresses are positive in tension and fluid pressures are positive in compression.

For the situation that the capillary stress are taken as the internal driving force ,the effective stress σ_e can be written as:

$$\sigma_e = \sigma - \kappa S \sigma_{cap} I \qquad (17)$$

Where S is the saturation fraction, σ_{cap} is the capillary stress in the pore fluid. The effective force σ_e can be used in Eq.(11) on the macroscale as load $\sigma(t)$ to calculate the deformation of the cement system.

3 Materials & methods

Portland cement (CEM I 42.5N) was used. The Portland cement had Blaine fineness 431 m^2/kg and calculated Bogue composition of C_3S 57.5%, C_2S 11.8%, C_3A 8.2%, and C_4AF 9.1%. Silica fume was added in slurry form, 10% by binder weight. The w/c ratio of the both pastes was 0.3. Cement paste was mixed in a 5 l epicyclic Hobart mixer. Demineralized water was mixed with the admixtures and added in two steps to ensure homogeneity. Total mixing time from first water addition was 3 minutes. The specimens were cured at 20 ℃ for at least one week.

3.1 Autogenous deformation

Cement paste was cast under vibration into tight plastic tubes (low density polyethylene plastic, LDPE), which were corrugated to minimize restraint on the paste. The length of the samples was approximately 300 mm and the diameter 25 mm. The specimens were placed in a dilatometer and immersed into a temperature controlled glycol bath at 20±0.1℃. Three samples were tested simultaneously in the dilatometer, with a measuring accuracy of ±5 μstrain. Linear measurements were recorded every 15 minutes and started about half an hour after casting for the Portland cement paste and after about 4 hours of rotation for the BFS cement paste. A top view of the dilatometer setup is shown in Figure 2. The dilatometer frame consisted of two steel plates joined rigidly together by four solid invar rods (diameter 20 mm). Each specimen is, therefore, longitudinally supported by two parallel rods attached to the steel plates. The specimens were gripped by coil springs at one end, while the rest could slide freely on the rods, which were lubricated by the glycol bath. The longitudinal deformation was measured at the free end by a LVDT displacement transducer. A detailed description of the dilatometer is provided in [13]. The corrugated mould enables to measure the linear deformations from the paste volume when it was in a fluid state. The ratio between the length and volume change was found to be 1.85 mm/ml [14]. The corrugated moulds were specially designed to minimize restraint on the paste. A maximum restraint force of 0.5 N (corresponding to a stress of 0.001 MPa) on the paste was measured [14] for a deformation of 10,000 μstrain. For comparison, it is noticed that the forces acting on the paste before setting are of the magnitude of the atmospheric pressure, i.e. about 0.1 MPa. The moulds are watertight: water loss from a tube filled with water kept at 20℃ and RH close to 0%, for one week, was about 0.04 g, corresponding to 0.03% of the water content[14] .

3.2 Elastic modulus

The elastic modulus in compression (secant modulus at 30% of the compressive strength) was measured after 1, 3 and 7 days of sealed hardening on cement paste prisms, 40×40×160 mm^3. The prisms were cast into temperature-controlled steel moulds and cured at 20℃. However, due to time constrains, in this paper, the elastic modulus was simulated by HYMOSTRUC.

3.3 Internal relative humidity

About 10 g of fresh cement paste was cast into the measuring chamber of two Rotronic hygroscope DT stations equipped with WA-14TH and WA-40TH measuring cells (Figure 1). Each station was equipped with a Pt-100 temperature sensor and a DMS-100H RH sensor. The RH sensors contain an electrolyte whose electrical impedance depends on the ambient RH. The RH stations were placed inside a temperature controlled room at 20±0.1℃. The RH and temperature in the samples were measured every 15 minutes for a period of about 1 week after water addition.

Figure 1 Rotronic station for RH measurement

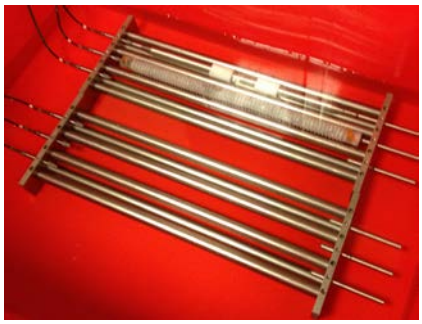

Figure 2 Dilatometer for autogenous deformation

4 Results and discussions

4.1 Elastic Modulus

Figure 3 shows the elastic modulus as a function of age for an ordinary Portland cement paste and a Portland cement paste with a 10% slilica fume replacement. The starting time of the test was taken equal to the mixing time.

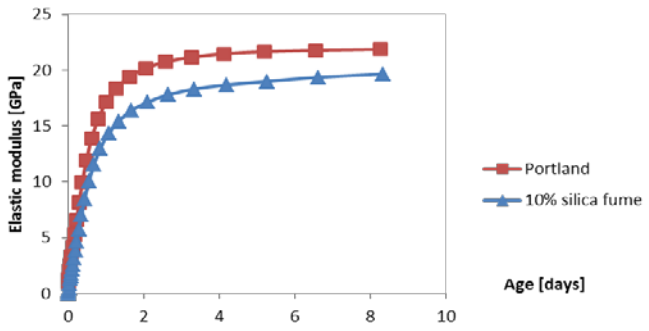

Figure 3 Elastic modulus as a function of age

4.2 Internal relative humidity

Internal RH of the cement pastes was measured on a sample for a period of at least 7 days. The development of internal RH, i.e. pore RH, with hydration time is provided in Figure 4. The starting time is the mixing time.

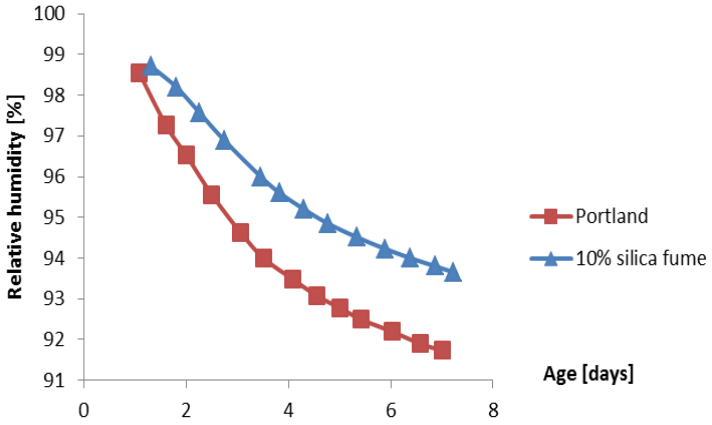

Figure 4 Internal RH as a function of age for the cement pastes

4.3 Autogenous Deformation

Figure 5 shows the measured autogenous deformation as a function of age for the ordinary Portland cement pastes and Portland cement paste with a 10% slilica fume replacement. The starting time is the final setting time because before that time, the specimens were on a rotation machine to avoid bleeding. The final setting time of the ordinary Portland cement was 5 hours and the Portland cement paste with 10% silica fume is 5 and half hours. In Figure 5, a fast shrinkage can be noticed after final setting, and after a short period of swelling the cement pastes started to shrink steadily. During this period other mechanisms play a role and can be introduced to explain the phenomenon of the fast shrinkage and swelling. A key issue in this respect is fact that the hydrating particles still do not touch each other resulting in a situation where no resistance can be built up against the internal capillary stresses. This is, therefore, called the plastic phase. In this paper, the simulation work will start after the swelling.

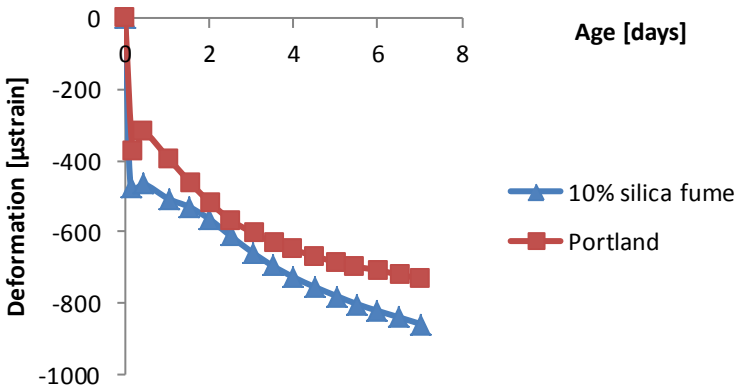

Figure 5 Measured autogenous deformation of cement pastes as a function of age

4.4 Modeling result

The calculation model based on the theory presented in this paper was used to simulate the autogenous shrinkage of hydrating cement paste after swelling . Figure 6 and Figure 7 show the calculated results and also show the measured autogenous deformation of ordinary Portland cement and Portland cement paste with 10% silica fume, after swelling, as a function of age. The deformation is calculated after the peak of the swelling and time 0 is the final setting time.

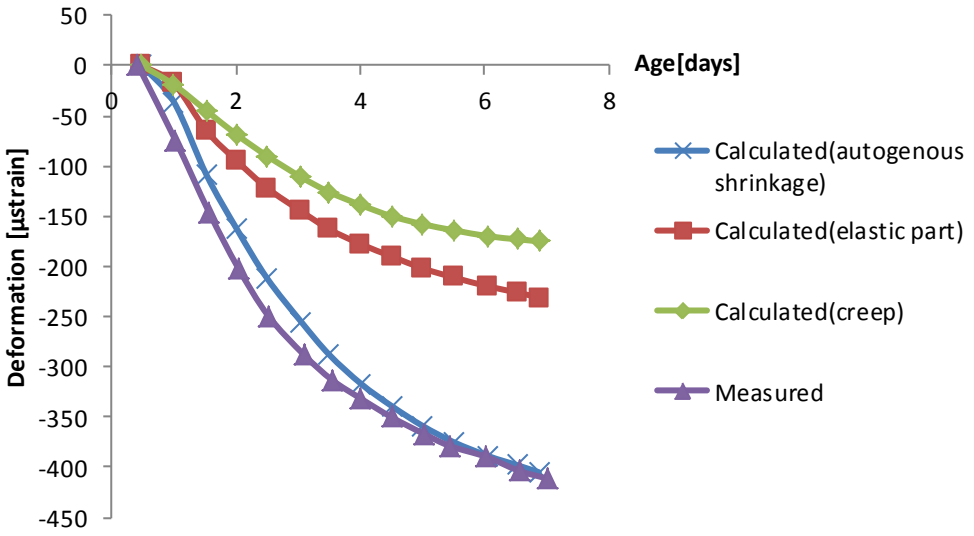

Figure 6 Measured and calculated autogenous deformation of ordinary Portland cement paste after swelling

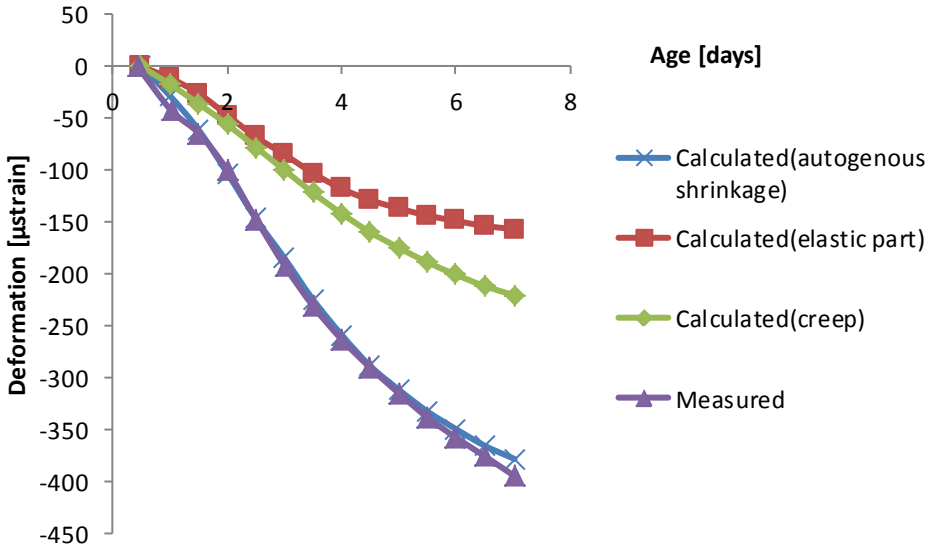

Figure 7 Measured and calculated autogenous deformation of Portland cement paste with 10% silicafume after swelling

5 conclusion

A novel model for autogenous deformation, including elastic and plastic parts, using consistently effective stresses was presented and experimentally validated. Application of the presented model was don on two numerical examples, and results were compared with experimental tests of cement paste strains measured from a Portland cement with and without 10% silica fume.

The examples confirmed that some additional autogenous strains, observed in experiments, that cannot be explained by the elastic deformation, could be very well attributed to the creep strains caused by the capillary stress of the hydrating system. But the existing model can only explain the autogenous shrinkage phenomenon after having passed the short time swelling.

Other mechanisms must be introduced when modelling swelling, e.g. hydration dispersion and crystalline pressure are the two principal mechanisms have often been mentioned[15].

In a research program to come, more attention will be paid to the autogenous deformation before the peak of the short time swelling, the objective is to explain the autogenous deformation more systematically and simulate it more accurately.

References

[1] van Breugel K. (2001) Numerical modelling of volume changes at early ages - Potential, pitfalls and challenges, Mater Struct 34(239): 293-301

[2] Lura P (2003) Autogenous deformation and internal curing of concrete . PhD Dissertation, Delft University of Technology.

[3] Day RL and Gamble BR (1983) The effect of changes in structure on the activation energy for the creep of concrete, Cem and Concr res 13:529-540

[4] Koenders E.A.B(1997), Simulation of volume changes in hardening cement-based materials, PhD Dissertation, Delft University of Technology.

[5] Bangham, D.H. and Maggs, F.A.P. (1944), The Strength and Elastic Constants of Coal in Relation to their Ultra-fine Structure, The British Coal Utilisation Research Association, The Royal Institution, London.

[6] Bazant, Z.P. and Wittmann, F.H. (1982), Creep and Shrinkage in Concrete Structures, John Wiley & Sons.

[7] Geiker M.R., Bentz D.P. and Jensen O.M., Mitigating Autogeneous Shrinkage by Internal Curing, High-Performance Structural Lightweight Concrete, ACI SP 218, pp. 143-148, 2004.

[8] Bentz, D. P. and Garboczi, E.J. (1991), Percolation of Phases in a Three-Dimensional Cement Paste Microstructural Model, Cement and Concrete Research ,21, 325-344

[9] Polivka M and Best CH (1960) Investigation of the problem of creep of concrete by Dorn's method . Springer, 39th Annual Meeting of the Highway Research Board, Washington January 1960

[10] Wittmann F (1971) Kriechverformung des Betons unter statischer und unter dynamischer Belastung, Rheologica Acta10:422-428

[11] Wittmann F and Klug P (1971) Zum zeitlichen Verlauf des Kriechens von ZEmentstein und Beton, Rheologica Acta 7:93-95

[12] Gawin D Pesavento F and Schrefler BA (2007) Modelling creep and shrinkage of concrete by means of effective stresses, Mater Struct 40:579-591

[13] Jensen OM and Hansen PF (1995) A dilatometer for measuring autogenous deformation in hardening Portland cement paste, Mater Struct 28(181): 406-409

[14] Jensen OM (1996) Dilatometer – further development, Building Materials Laboratory, The Technical University of Denmark, Lyngby, Denmark.

[15] Budnikov and PPStrelkov MI(1966) Some recent concepts on portland cement hydration and hardening, Highway Research Board Special Report,90